Adsorption 3, 41–54 (1996)

Convection-Diffusion of Solutes in Dynamic Media

DURGESH S. VAIDYA, J.M. NITSCHE, S.L. DIAMOND AND DAVID A. KOFKE
Department of Chemical Engineering, State University of New York at Buffalo, Buffalo, NY 14260-4200, U.S.A.

Abstract. We investigate convective-diffusive transport of a solute through a medium with properties that can be externally modulated in space and time. In particular, we focus on the effect of a front—a sharp transition in the convective velocity (v) and diffusivity (D)—on the evolution of the solute concentration profile. Numerical results show that by suitably moving the front during the process an anti-dispersive effect may be realized, in which the solute accumulates in a thin region close to the moving boundary. Our computations take into account the realistic case of a front having a small but finite thickness, and we find that the width of the concentration profile scales as $(1/\sqrt{\mathrm{Pe}})$, where Pe is the Péclet number. This is in sharp contrast to the $1/\mathrm{Pe}$ scaling observed for the ideal case of the singular front assumed in previous work. The effect of the thickness of the front and the magnitude of the drop in v and D, on the solute concentration profile has also been studied. These results are relevant in order to implement and optimize protocols that apply an externally controlled moving boundary for the purpose of separation.

We also present experimental results characterizing solute transport across a stationary front, expected to display many features needed in a model for moving fronts. The concentration profile of electrophoretically mobile BSA-FITC within the boundary layer at a polyacrylamde gel-buffer interface were visualized by epifluorescence microscopy. Measured boundary layer thickness exceeded that predicted for even a finite interface, indicating that the length scale associated with real boundaries is relevant to the modeling problem.

Keywords: liquid crystals, moving bed system, simulation, purification

1. Introduction

Over the last decade there has been a considerable effort to make separation columns more dynamic and flexible. One approach has been to introduce changes in the composition of the mobile phase during its elution. This principle formed the basis of moving boundary electrophoresis (Chrambach, 1985; Brzezinski et al., 1989). These modifications are limited to liquid phase separations, particularly when the retention behavior or mobility of the solutes is strongly dependent on the pH of the mobile phase. Another approach is to make the stationary phase—rather than the mobile phase—dynamic and tunable via, for instance, an externally applied electric field. A suitably applied ac or dc electric field can augment the conventional driving force of a process to enhance the efficiency of the system in terms of purity, degree of separation, and yield (Muralidhara, 1994). Alternatively, an electric field is capable of inducing changes in the electrochemical properties of a stationary phase, thereby introducing a driving force for separation that would be otherwise absent in a process. One of the earlier steps towards modifying the behavior of stationary phases through applied voltages was in electromodulated ion exchange chromatography by Ghatak-Roy and Martin (1986). The technique has undergone several developments and a more recent version of this method has been discussed by Deinhammer et al. (1995). In this set-up, nonporous glassy carbon spheres are used as the stationary phase. Modulation of the surface charge of the spheres via an external voltage controls the retention behavior of the mobile solutes during elution, thereby leading to improved resolution in a mixture of ten aromatic sulfonates.

In the field of electrophoresis, the use of multiple electrode voltages for separation of DNA molecules of sizes greater than 50 kilobases and up to 2 megabases

has been demonstrated by Chu et al. (1986). Sauer et al. (1995) have performed a theoretical study of the effect of axial and orthogonal auxiliary electric fields on the residence time of small, non-interacting solutes undergoing laminar flow through a rectangular channel. The time required to achieve a resolution of 2.0 in a binary mixture was seen to decrease when the fields were turned on compared to when they were shut off.

One-dimensional electrophoresis facilitates good resolution but is limited to small throughputs. Chromatography, on the other hand, can handle larger throughputs but cannot compete with electrophoresis for resolution. With the introduction of counteracting chromatographic electrophoresis (CACE) by O'Farrell (1985), the features of chromatography and electrophoresis were combined. CACE uses opposing electric and convective fields to focus proteins at the boundary separating two gels of different internal porosity. An extension of this version for continuous operation has been developed by Ivory and Gobie (1990). The quantitative focusing limits for this operation have been discussed by Raj (1994). In contrast to the time dynamic nature of separations discussed in the previous paragraph, CACE is an example of separations using a spatially varying (composite) stationary phase. A major advantage of this technique is that in addition to isolating the target protein, it is concentrated by a factor of the order of 10–1000.

Electric fields are being introduced in the area of membrane separations too. Grimshaw et al. (1989) have fabricated polyacrylamide and polymethacrylic acid membranes with permeabilities that can be chemically and electrically modulated over a period of time. Winnick (1990) has discussed the advantage of replacing the pressure gradient with an electric field for separation of an ionizable gaseous solute from other uncharged components. For a species of valency ± 2, a voltage of 60 mV can maintain the same concentration difference that would require 100 atm for an uncharged species. Bhaskar et al. (1985) and Ly and Cheng (1993) have synthesized liquid crystalline membranes with an electrically controlled permeability. On application of an electric field the microstructure of the membrane undergoes a change that leads to an increase in the flux across the membrane. Such membranes are important in controlled drug delivery applications.

Liquid crystals (LCs) are thin, rigid, rod-like molecules with a tendency to align themselves more or less parallel to each other. This spontaneous alignment makes the medium anisotropic in optical, electrical, and transport properties (de Gennes and Prost, 1993). Moreover, the direction of common alignment can be modulated by the application of an external electric field. In a tubular column filled with a LC medium, the molecules could be interchangeably made to align parallel and perpendicular to the tube axis. We will refer to the former microstructure as the parallel mode and the latter as the perpendicular mode.

A change in microstructure of a LC stationary phase results in a change in the velocity and diffusion coefficient of a mobile solute. By changing the distribution of LC molecules between parallel and perpendicular (including intermediate configurations), in principle, the solute velocity can be controlled in space *and* time between a maximum value ($v_{\parallel}$) and a minimum value ($v_{\perp}$). This tunability is a unique feature of such materials and the prospect of using it as the basis for separations is explored here.

As discussed below, a high degree of anisotropy (as expressed by the ratio $v_{\perp}/v_{\parallel}$) is a desirable feature of a tunable separation medium. Liquid crystal polymers exhibit large anisotropy but also require times of the order of hours to respond to the presence of an electric field. Low molecular weight liquid crystals have small response times ($\sim$200 msec.) to an electric field but do not have large anisotropies ($v_{\perp}/v_{\parallel} \sim$ 0.8–0.9). Synthesis of liquid crystalline materials with adequately low response times ($\sim$10 sec.) and a sufficiently high degree of anisotropy ($v_{\perp}/v_{\parallel} \sim 0.5$) would greatly aid the development of a tunable separation device.

At present, we are concerned with developing protocols for operation of a separation device that can exploit the properties of a tunable medium. We would like to demonstrate that significant advantage can be gained from dynamically controlling—in space and time—the transport properties of a separation medium. In a related work, we have shown that the most desirable configuration involves a series of adjacent parallel and perpendicular modes (Vaidya et al., 1996). This distribution gives rise to fronts—thin regions in which the alignment of the liquid crystals changes from parallel to perpendicular and vice versa. Of special interest in this paper is the use of moving fronts to concentrate specific solutes. Thus, it is important to understand theoretically the process of solute mass transfer through such structures.

Convection-diffusion mass transfer in composite media with piecewise constant transport properties has been extensively modeled on the basis of the self-adjoint operator formalism developed by Ramkrishna and Amundson (1974), which was later extended by Locke and Arce (1993a) and Locke et al. (1993). Although this method gives the exact analytical solution to the governing equations of mass conservation, there are two limitations to its practical applicability in the processes we consider here. First, the method is known to converge slowly in the regime of large Péclet numbers Pe (defined in Eq. (16)). This is a problem since most practical separations are designed and operated such that convection dominates over diffusion, because this allows for a smaller size of the column and better resolution of the solutes. To overcome the computational difficulties encountered in modeling high-Pe separation operations, a singular perturbation analysis approach for solute transport in a medium with discontinuous transport properties was introduced by Vaidya et al. (1995). Their study was restricted to the case of a singular (zero width) interface at a fixed location within the column. For the case where the solute velocity upstream of the interface was faster than that downstream, it was observed that the concentration of the solute rises within a thin boundary layer (thickness $\delta_{\text{sing}}/L = O(1/\text{Pe})$) upstream of the front to satisfy the requirement of the continuity of flux at the surface of discontinuity (see Fig. 1). The second limitation has to do with the fact that fronts, in reality, are not singular surfaces across which transport properties suffer discontinuities, but rather smooth transition regions of small but finite width. Indeed, in liquid crystal media, elastic resistance of the molecules would produce a transition layer of thickness δ_f of order 100 μm (de Gennes and Prost, 1993).

Our purpose here is to explore the consequences of this finite thickness for solute transport. After setting up the governing equations in Section 2 and our experimental technique in Section 3, we present in Section 4 results for two physical circumstances, namely (1) steady mass transfer through a stationary front, and (2) transient mass transfer near a moving front. For (1), both theoretical and experimental results show that the solute concentration changes over a length scale considerably larger than the $O(1/\text{Pe})$ boundary layer thickness predicted for a discontinuous medium. For (2), finite thickness of the transition zone has a profound influence on the local solute concentration. In the process of exploring this, we demonstrate the possibility of concentrating solutes near a moving front, and identify the scaling of the resulting solute peak with the Péclet number.

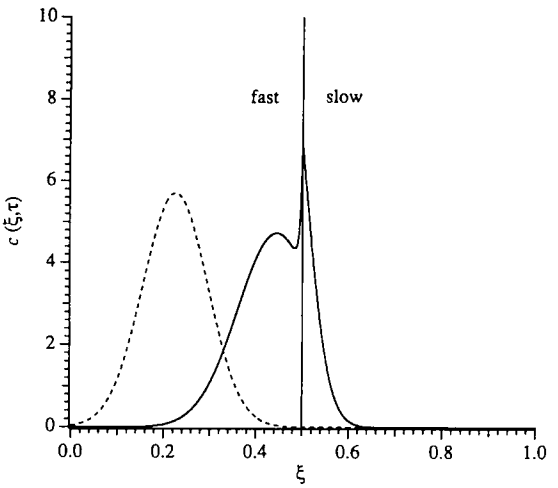

Figure 1. Increase in concentration of solute within the boundary layer on migrating from a fast into a slow domain across a stationary front. The ratio of upstream to downstream transport properties is 0.50. The variables (ξ, τ) are as defined in Eq. (15). The dashed curve is the initial distribution and the solid curve is the distribution at a dimensionless time $\tau = 0.17$. The vertical line represents the front.

2. Theory for a Moving Front

2.1. *Principle*

As Fig. 1 illustrates, when a solute undergoes convection-diffusion across an interface into a domain where its convective velocity (and diffusivity) decrease, there is a sharp rise in its concentration near the interface. For an interface with a position that is fixed in time, this increase in concentration is restricted to the short time scale over which the solute passes through the front. Afterwards, the peak spreads out owing to diffusional effects. In the present work, we consider a column containing a composite material which is dynamic and tunable such that the boundary of demarkation between the domains can be made to move at an independently controlled velocity relative to the solute. The solute could then be made to experience the presence of the interface for much larger time scales leading to a progressive concentration increase at the front. Taking the upstream velocity as $v_{\parallel}$ and that downstream as $v_{\perp}$ ($v_{\parallel} > v_{\perp}$), three possibilities arise naturally for the

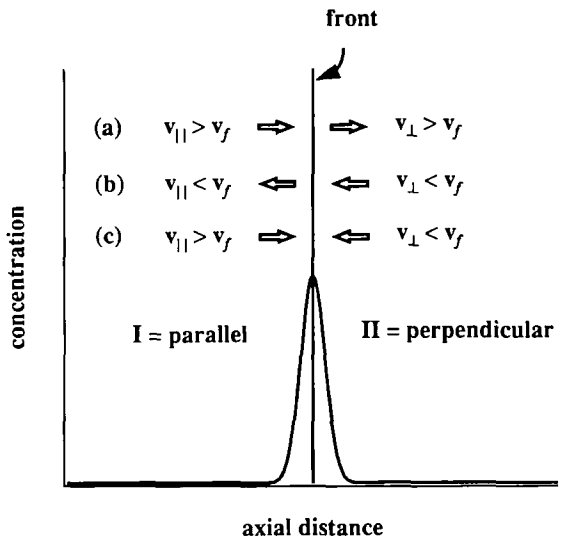

Figure 2. Illustration of the principle of dynamic separations using a moving front. When the front moves with a velocity that is intermediate to the upstream (high) and the downstream (low) value, there will be progressive accumulation of the solute at the moving boundary.

choice of the velocity of the front (v_f): a) $v_f < v_\perp < v_{||}$, b) $v_\perp < v_{||} < v_f$ and c) $v_\perp < v_f < v_{||}$. Figure 2 illustrates the velocity vectors relative to the moving front for these three cases. Case a) is similar in qualitative behavior to the stationary front (corresponding to the special case $v_f = 0$) and, therefore, suffers from the same limitation of a short time scale of interaction between the solute and the front. The same is true of case b). In case c) there is incoming flux at the interface from both upstream and downstream domains. In the absence of substantial diffusion, mass conservation would require that the concentration continuously increase within a thin layer at the interface. Eventually, the entire solute content would be trapped within the boundary layer. As the front moves towards the exit, the solute is eluted out. For large values of Pe, the height and width of the peak in the solute concentration scale with Pe and 1/Pe respectively, as can be shown by generalizing the boundary layer analysis of Vaidya et al. (1995) for discontinuous media—see Vaidya et al. (1996). As we shall demonstrate below, however, small but finite width of the front changes the situation dramatically.

2.2. *Mathematical Formulation*

Consider transient, one-dimensional convective-diffusive transport of a solute where the convective

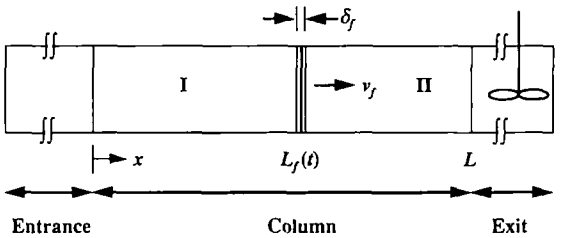

Figure 3. Column containing a dynamic medium comprising two domains of different transport properties. The transition zone between the two domains can be independently controlled to move with a constant velocity v_f. The thickness of the zone is δ_f and its mean position at time t is $L_f(t)$.

velocity (v) and the diffusivity (D) are uniform except for a transition layer centered about the plane $x = L_f$ (Fig. 3). The concentration field $c(x, t)$ is governed by the Brownian transport equation

$$\frac{\partial c}{\partial t} = \frac{\partial}{\partial x}\left[D(x,t)\frac{\partial c}{\partial x}\right] - \frac{\partial}{\partial x}\left[v(x,t)c\right]. \qquad (1)$$

Throughout this paper, we will use superscript $i = \mathrm{I}$ to distinguish the left (upstream) region ($0 \le x \le L_f$) where $D = D^{\mathrm{I}}$ and $v = v^{\mathrm{I}}$, and $i = \mathrm{II}$ for the right-hand side (downstream) domain ($L_f \le x \le L$) where $D = D^{\mathrm{II}}$ and $v = v^{\mathrm{II}}$. The line of demarkation between the upstream and downstream domains, referred to as the front, can itself be made to move with a uniform velocity v_f. The location of the front at a given instant in time t is then given by:

$$L_f(t) = L_{f0} + v_f t \qquad (2)$$

where L_{f0} is the position of the front at $t = 0$. The case of a stationary front (Vaidya et al., 1995) is recovered by setting $v_f = 0$ (see Section 4.1).

We assume that at time $t = 0$ the column contains a prescribed initial distribution of the solute. At all positive times, there is no solute flux entering the column from upstream. The section of the column beyond $x = L$ is both infinite in length and well-mixed, so that Danckwerts' boundary conditions hold (Danckwerts, 1953; Novy et al., 1990). Therefore,

$$c(x, 0) = f(x), \qquad (3)$$

$$-D^{\mathrm{I}}\frac{\partial c(0,t)}{\partial x} + v^{\mathrm{I}}c(0,t) = 0, \quad t > 0 \qquad (4)$$

$$\frac{\partial c(L,t)}{\partial x} = 0, \quad t > 0. \qquad (5)$$

For cases where the transition from downstream transport properties occur over a region of small but finite thickness δ_f, we utilize the form

$$D(x,t) = \begin{cases} D^{\mathrm{I}}, & x < L_f(t) - (\delta_f/2) \\ D^{\mathrm{II}}, & x > L_f(t) + (\delta_f/2) \\ D^{\mathrm{II}} + (D^{\mathrm{I}} - D^{\mathrm{II}})\cos^2[\theta(x,t)], & \\ \qquad L_f(t) - (\delta_f/2) < x < L_f(t) + (\delta_f/2) & \end{cases} \tag{6}$$

where $\theta(x,t)$ refers to the orientation of the LC molecules with respect to the axis of the column. The value $\theta = 0$ refers to the parallel mode while $\theta = \pi/2$ refers to the perpendicular mode. The orientation distribution in the transition zone was approximated by the smooth functional form

$$\theta(x,t) = \frac{\pi}{2}(3\eta^2 - 2\eta^3) \tag{7}$$

where η is given by:

$$\eta = \frac{x - L_f(t) + (\delta_f/2)}{\delta_f}. \tag{8}$$

The orientation distribution in Eq. (7) ensures that the solute diffusivity within the transition zone reaches its upstream and downstream values with zero slope. The velocity change $v(x,t)$ is approximated by an analogous formula.

For the case where the change from upstream to downstream transport properties occurs as a discontinuity, we introduce upstream and downstream concentrations $c^i(x,t)$ $(i = \mathrm{I}, \mathrm{II})$, for which Eq. (1) reduces to the constant coefficient equation

$$\frac{\partial c^i}{\partial t} = D^i \frac{\partial^2 c^i}{\partial x^2} - v^i \frac{\partial c^i}{\partial x}, \qquad i = \mathrm{I},\ \mathrm{II}, \tag{9}$$

and Eqs. (3)–(5) become:

$$c^i(x,0) = f^i(x), \qquad i = \mathrm{I},\ \mathrm{II} \tag{10}$$

$$-D^{\mathrm{I}} \frac{\partial c^{\mathrm{I}}(0,t)}{\partial x} + v^{\mathrm{I}} c^{\mathrm{I}}(0,t) = 0, \qquad t > 0 \tag{11}$$

$$\frac{\partial c^{\mathrm{II}}(L,t)}{\partial x} = 0, \qquad t > 0. \tag{12}$$

The existence of a sharp interface at $x = L_f(t)$ introduces the need for two additional conditions to piece together the as yet unrelated concentration fields $c^{\mathrm{I}}(x,t)$ and $c^{\mathrm{II}}(x,t)$. The appropriate conditions are the requirements of local equilibrium and continuity of flux at $x = L_f(t)$ for all positive times, *viz*

$$c^{\mathrm{I}} = K_{\mathrm{eq}} c^{\mathrm{II}} \tag{13}$$

$$-D^{\mathrm{I}} \frac{\partial c^{\mathrm{I}}}{\partial x} + (v^{\mathrm{I}} - v_f) c^{\mathrm{I}} = -D^{\mathrm{II}} \frac{\partial c^{\mathrm{II}}}{\partial x} + (v^{\mathrm{II}} - v_f) c^{\mathrm{II}}. \tag{14}$$

In order to solve Eqs. (1), (3)–(5) numerically, they are recast in a dimensionless form in which the length ξ is measured in units of L and time τ is measured in units of $\bar{v}/L$. The following non-dimensional groups then arise:

$$\xi = \frac{x}{L}; \qquad \tau = \frac{t\bar{v}}{L}; \tag{15}$$

$$\mathrm{Pe} = \frac{\bar{v}L}{\bar{D}}; \qquad \epsilon = \frac{1}{\mathrm{Pe}}; \tag{16}$$

$$\phi^i = \frac{D^i}{\bar{D}}; \qquad \mu^i = \frac{v^i}{\bar{v}}. \tag{17}$$

here $\bar{D}$ and $\bar{v}$ respectively denote the characteristic values for the diffusivity and velocity. Let the front be located at L_{f0} at time $t = 0$ such that the entire initial solute distribution is to its upstream side. The interval of time required for complete pile-up of the solute against the front (t_p) is the time required for the lagging end of the solute distribution, located at a distance, say δL_{f0}, away from the interface, to convect to the front i.e.,

$$(v^{\mathrm{I}} - v_f)\, t_p = \delta L_{f0}. \tag{18}$$

This corresponds to a dimensionless time interval given by:

$$\tau_p = \frac{\delta\xi_{f0}}{\mu^{\mathrm{I}} - \mu_f} \tag{19}$$

where $\delta\xi_{f0} = \delta L_{f0}/L$ and $\mu_f = v_f/\bar{v}$. From Eq. (19), it can be seen that in order to concentrate the solute in the shortest time the front should be moved with a velocity equal to the (slower) downstream velocity of the solute. Moving the front with a velocity that is larger (but still $< v_{\|}$) would also produce the effect of progressive accumulation, but it would require a longer time of operation.

We choose the upstream transport properties as the reference values, i.e., $\bar{D} \equiv D^{\mathrm{I}}$ and $\bar{v} \equiv v^{\mathrm{I}}$ and define the following variables:

$$\alpha = (D^{\mathrm{II}}/D^{\mathrm{I}}) \tag{20}$$

$$\beta_f = (\mu_f/\mu^{\mathrm{I}}) \tag{21}$$

The parameter α quantifies the anisotropy of the medium for the solute and the parameter β_f represents the dimensionless velocity of the front relative to the reference value.

2.3. *Computations*

The finite difference scheme QUICKEST (Leonard, 1979) was employed for solving the convection-diffusion problem, cast in dimensionless form, for a smooth transition between zones I and II (Eq. (1), and Eqs. (3)–(5)). In this method the value of concentration at each grid wall is given by a central difference corrected by a term proportional to the upstream-weighted curvature. This hybrid strategy avoids the stability problems of central differencing and reduces the inaccuracies of numerical diffusion associated with upstream differencing. Accurate resolution of the concentration within the thin region where the parallel mode (upstream) changes into the perpendicular mode (downstream) was accomplished with a mesh size $\Delta\xi$ of 5.0×10^{-5}; the transition zone was thus discretized over 20 nodes for $\delta_f = 100$ μm and 200 nodes for $\delta_f = 1000$ μm. A uniform mesh of this size, covering the entire column of length $L = 10$ cm, would require 200,000 nodes and create tremendous demands for memory and cpu time. A majority of the nodes are, in fact, not essential as the initial solute concentration profile is non-zero over only a small fraction of the length of the column. Therefore we employed a smaller, traveling grid covering only the region where the initial concentration profile is significant and moving with the same speed v_f as the front. For a Gaussian initial distribution, about 99.99% of the mass is included within four standard deviations (4σ) from the mean. We therefore chose the traveling grid to be of length $L_x \sim 16\sigma$, centered initially on the mean.

For purpose of illustration, the velocity in each domain is assumed to be proportional to the diffusivity as is the case for small, non-interacting solutes. As a result the Péclet number in the upstream domain is the same as that in the downstream domain. For calculating the profile at a particular Péclet number, the velocity of the solute in each domain is thus given by $v^i = \mathrm{Pe}\ D^i/L$ or $\mu^i = \phi^i$. Note that our computational method is equally applicable to situations where this is not the case.

3. Experiments for a Stationary Front

In Section 2.1, we established the working principle of progressive accumulation of a solute at a moving front. For many applications it is unnecessary to know the details of concentration changes within a thin boundary layer at an interface. The continuity of flux is usually modeled macroscopically in terms of a lumped "mass transfer coefficient" term. In our application, the entire solute content piles up near the interface, and resolving the details of concentration gradients within this layer therefore becomes essential. Prior to implementing the protocol with moving fronts, it is worthwhile to understand concentration boundary layer dynamics at a stationary interface. Although data for self-diffusion in LCs is abundant (Krüger, 1982), experimental values for solubility limits and mobilities of electrically active solutes is limited. Therefore in studying solute concentration gradients in the interfacial region, we have chosen to work with polyacrylamide (PA) gels. These materials are extensively used for electrophoretic separations of biological molecules, and the transport properties of a variety of solutes through them are known in literature. Experiments were limited to a study of steady convection-diffusion through a stationary interface.

3.1. *Materials and Method*

Figure 4 shows the experimental set-up for studying the boundary layer transport of a solute through a stationary front using sodium dodecyl sulfate—polyacrylamide gel electrophoresis (SDS-PAGE). First, a 7% polyacrylamide sample was prepared in a glass capillary of 1 mm ID and length 10 cm. The gel matrix was 3 cm in length and in the center of the capillary. The rest of the tube was then filled with the electrophoretic buffer on both sides of the gel. The junction between the clear buffer fluid and the gel forms the stationary interface. The solute sample consisted of bovine serum albumin conjugated with fluoroscein isothiocyanate (BSA-FITC) at a concentration of 26 μg/ml (0.38 nM/ml).

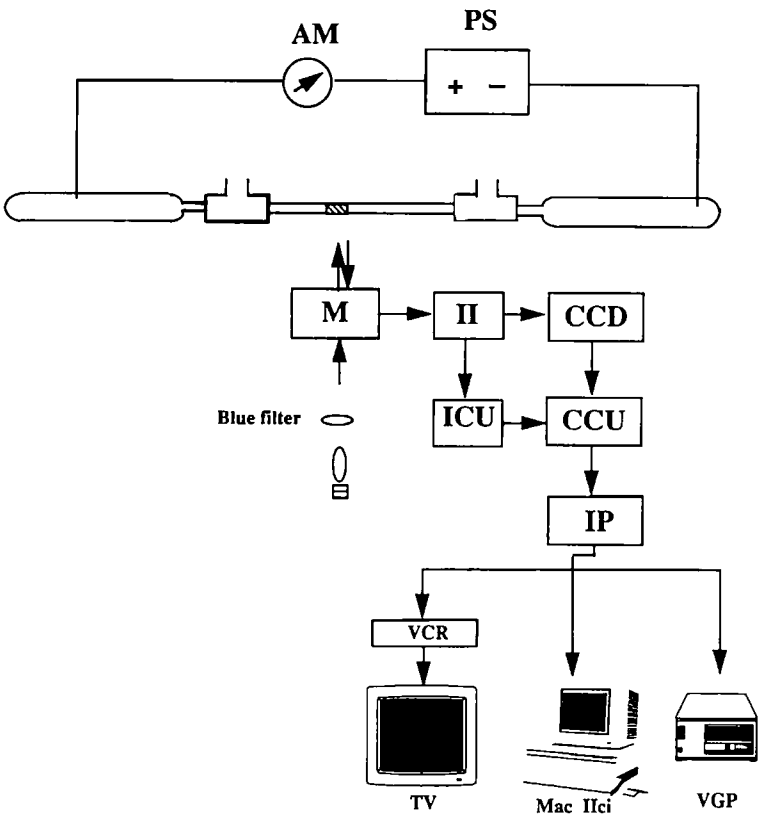

Figure 4. Experimental set-up for the study of boundary layer dynamics. M—microscope, II—image intensifier unit, CCD—charge coupled diode camera, ICU—image control unit (GenIIsys), CCU—camera control unit (GenIIsys), IP—image processor, VGP—video graphics printer. The hatched area in the middle of the capillary indicates the position of the PA gel.

The right reservoir was loaded with the solute sample. On application of an electric field (100 V across the capillary), BSA-FITC from the reservoir migrates electrophoretically towards the positive electrode and this constitutes a constant flux of the solute coming into the buffer-gel front. Constant input of the solute at the interface ensured that the boundary layer formed remained stable for long periods of time and concentration changes can then be observed under fully developed steady state conditions. Concentration detection and quantification were carried out using epifluorescence video microscopy. A Nikon inverted microscope (4X objective) was used for epifluorescence visualization with blue excitation (490 nm) and green emission (510 nm). The fluorescence emission was directed toward an image intensified (GenIIsys)—charge coupled diode (CCD-72) camera assembly (Dage-MTI). A Hamamatsu Argus-10 Image Processor was used for noise reduction by averaging the image over 16 frames. The data was recorded on 1/2″ videotape for digital image analysis (NIH Image 1.54) using a Quickcapture framegrabber (Data Translation) and a Macintosh IIci. The image of the uniform illumination on the upstream side of the front was used as the standard for normalizing the concentration curves.

4. Results

4.1. Stationary Front

We recall the two key premises in the boundary layer analysis by Vaidya et al. (1995) are that the column operates at a high Pe and that the change in microstructure occurs as a sharp interface. Under these conditions, the expression for the shape of the concentration profile within the boundary layer can be written as (Vaidya

et al., 1995):

$$c^{\mathrm{I}}(x) = c^{\mathrm{I}}_{\infty}\left[1 + \left(K_{\mathrm{eq}}\frac{v^{\mathrm{I}}}{v^{\mathrm{II}}} - 1\right) \times \exp\left(\frac{v^{\mathrm{I}}}{D^{\mathrm{I}}}(x - L_{f0})\right)\right]. \quad (22)$$

The above equation represents the steady state concentration distribution very near the interface for a continuous solute input of concentration c^{I}_{∞}. In our experiment, c^{I}_{∞} denotes the concentration of BSA-FITC in the bulk of the buffer far away from the interface. Neglecting any curvature effects at the junction of the buffer liquid and the PA gel, L_{f0} is the location of the interface and K_{eq} is as defined in Eq. (13). Taking the limit as one goes far away from the interface in Eq. (22), the ratio of the concentration of BSA-FITC at the interface to its value in the bulk of the buffer is given by

$$\frac{c^{\mathrm{I}}_{f}}{c^{\mathrm{I}}_{\infty}} = K_{\mathrm{eq}}\frac{v^{\mathrm{I}}}{v^{\mathrm{II}}}. \quad (23)$$

The external porosity of the gel sample used is 7%, so that $K_{\mathrm{eq}} = 1/(1 - 0.07)$ i.e., 1.07. The upstream domain is the buffer fluid and the downstream domain is the gel matrix; the ratio $v^{\mathrm{II}}/v^{\mathrm{I}}$ then is precisely the relative mobility of BSA-FITC in the gel. This value is known for a 7% PA gel and equals 0.5 (Gallagher and Smith, 1993). The macroscopically observed "concentration jump" $c^{\mathrm{I}}_{f}/c^{\mathrm{I}}_{\infty}$ in going from the buffer to the gel domain is evaluated from Eq. (23) and is found to be 2.15. The experimental value of 1.9 observed in Fig. 9 is 13% lower than the theoretical prediction.

Also relevant is the decay length associated with the concentration profile. This parameter is represented by the reciprocal of the coefficient in the exponential term in Eq. (22) and was calculated to be about 2 μm. This estimate differs vastly from the experimentally observed decay length of about 250 μm. The discrepancy stems from the fact that Eq. (22) has been derived assuming that the interface has zero width. In the experiment, the interface was observed to be of thickness 100 ± 4 μm and its mean thickness is marked by the two solid vertical lines in Fig. 5. Thus the transition between the two domains could be modeled as a continuous change in the velocity and diffusivity of BSA-FITC from the buffer to the gel matrix with $\delta_f = 100$ μm. The convection-diffusion of solute is governed by Eq. (1). Since the Pèclet number is large,

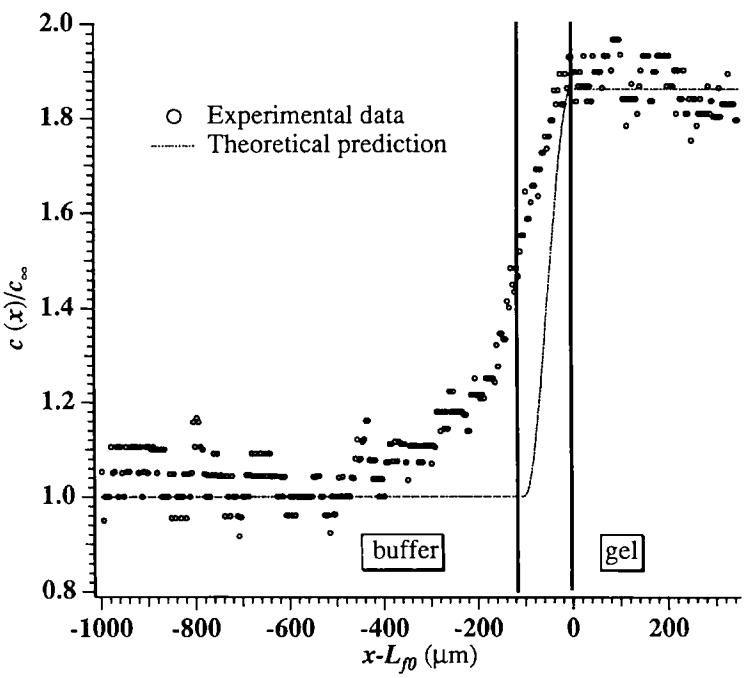

Figure 5. Concentration profile of BSA-FITC within the boundary layer at the buffer-PA gel interface. The two vertical lines indicate the thickness of the interface. The solid curve represents theoretical solution assuming a smooth transition of transport properties within the interface.

it is appropriate to neglect diffusion zone in Eq. (1), which then reduces to

$$\frac{d}{dx}[v(x)c(x)] = 0. \tag{24}$$

The solution to this equation subject to the condition that at $x = 0$, $c = c_\infty^{\mathrm{I}}$ and $v = v^{\mathrm{I}}$ is

$$c(x) = \frac{c_\infty^{\mathrm{I}} v^{\mathrm{I}}}{v(x)}, \tag{25}$$

which is a statement of continuity of convective flux through the transition zone. Equation (25) has the feature that the interval over which the concentration changes from c_∞^{I} to its downstream value coincides precisely with the thickness of the front (which is much greater than L/Pe). The dashed curve in Fig. 5 corresponds to Eq. (25) with the variation in the convective velocity represented algebraically by a form similar to Eq. (6). Whereas this behavior for a stationary front represents a simple static phenomenon, finite thickness of the front (inevitable in practical situations) has more interesting dynamical consequences for the case of the moving front.

4.2. *Moving Front*

The traveling mesh consisted of 2000 nodes, with a grid spacing $\Delta\xi = 5.0 \times 10^{-5}$ as mentioned before, and a time step of $\Delta\tau = 1.0 \times 10^{-6}$. In all the examples illustrated, the initial distribution of each solute was chosen to be a Gaussian with its mean located at $\xi = 0.05$ and a dimensionless standard deviation $\sigma/L = 0.007$. The mass content per unit cross sectional area is 1.0 g/cm^2. The values of the reference anisotropy α considered were 0.80 and 0.50. The former is based on the anisotropy in diffusion coefficients ($D_\perp/D_\parallel$) of methane in the LC *p*-methoxy-*n*-alkylazoxybenzene (Merck Licrystal Phase 5) as determined by Moseley and Loewenstein (1982). The latter is a value for a hypothetical LC. All other parameters are as indicated in figure captions. The interval of time to be simulated was chosen on the basis of Eq. (19).

Figures 6 and 7 show the evolution of the concentration profile for the solute for an operation in which the front is moved with its downstream velocity. Unless stated otherwise, all simulations are carried out at $\mathrm{Pe} = 10{,}000$, the initial location of the front is at $\xi_{f0} = 0.0775$ and the lagging end of the solute distribution is taken at $\xi = 0.0275$ to give $\delta\xi_{f0}$ a value

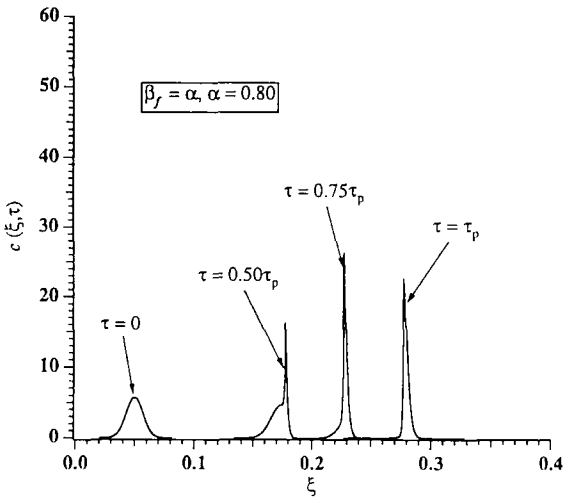

Figure 6. Numerical simulation of convection-diffusion of a solute with a moving front in a medium with a reference anisotropy of 0.80. The front moves with a velocity equal to the downstream velocity of the solute. The simulation interval τ_p is 0.25.

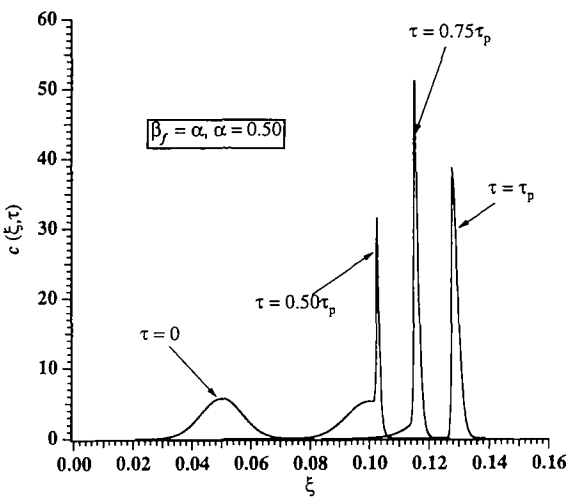

Figure 7. Same as Fig. 6, but for a reference anisotropy of 0.50 and a simulation interval of $\tau_p = 0.1$.

of 0.05. It is observed that long term interaction between the solute peak and the moving front causes a progressive accumulation of the solute very close to the interface. However, it can be seen that the maximum height of the solute increases upto a period of about 0.75 τ_p and decreases thereafter. We would like the concentration to increase continually as the solute moves from the entrance to the exit. The reason for the fall of peak height at intermediate times lies in the

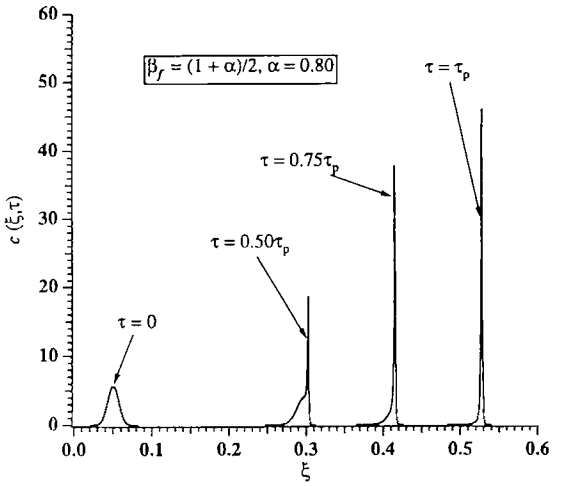

Figure 8. Numerical simulation of convection-diffusion of a solute with a moving front in a medium with a reference anisotropy of 0.80. The front moves with a velocity that is the arithmetic mean of the upstream and downstream values for the solute. The simulation interval τ_p is 0.50.

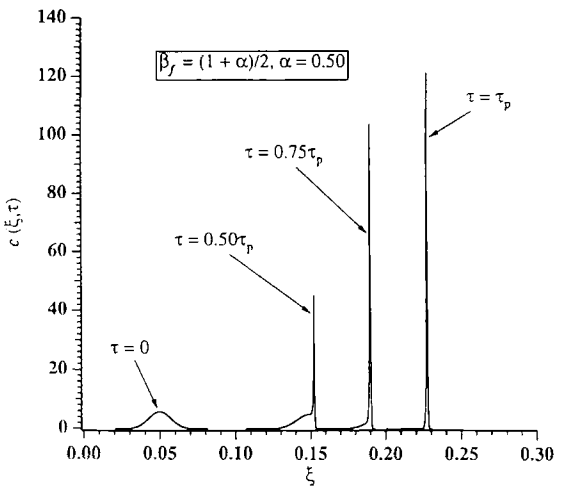

Figure 9. Same as Fig. 8, but for a reference anisotropy of 0.50 and a simulation interval of $\tau_p = 0.2$.

extreme choice of the front velocity and is discussed in detail in the next section. To overcome the undesirable effect of peak height reduction at large times, the velocity of the front was increased to a value that is the mean of the upstream and downstream values for the solute. As can be seen from Figs. 8 and 9, this protocol resulted in a continuous solute pile-up at the moving boundary although beyond a period of τ_p the peak height remained constant. This is because the concentration gradients at the interface get large

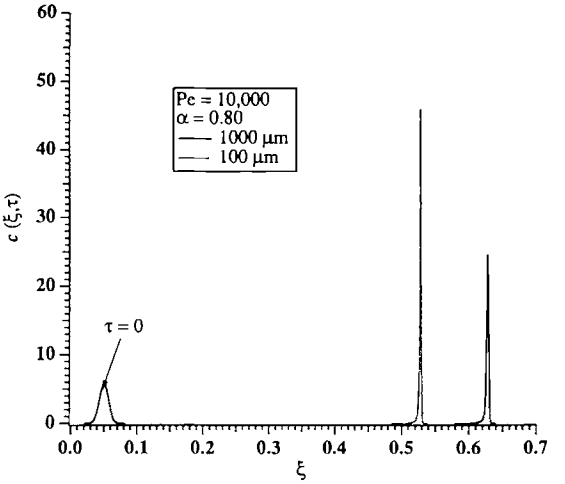

Figure 10. Effect of the thickness of the transition zone. The reference anisotropy of the medium is 0.80. The front moves with a velocity that is the arithmetic mean of the upstream and downstream values for the solute. The simulation interval τ_p is 0.50 for a transition zone thickness of 100 μm and 0.6 for that of 1000 μm.

enough such that the diffusional fluxes out of the front are in dynamic equilibrium with the convective fluxes into the interface. The peak height (or width) referred to hereafter refers to this final maximum value. The remaining results are presented for the case of the front moving with a velocity that is the arithmetic average of the upstream and downstream values for the solute i.e., $\beta_f = (1 + \alpha)/2$.

Having achieved the qualitative behavior of concentrating the solute in a sharp peak near the interface, a key quantitative issue arises, *viz* the relation of the peak height (or width) to the material properties of the medium—reflected in the thickness of the transition zone δ_f—and the operational parameters in the column—captured by the Péclet number Pe. Figures 10 and 11 show the solute concentration for a broader interface ($\delta_f = 1000\ \mu$m). The location of the mean of the transition zone was shifted from $\xi_{f0} = 0.0775$ to $\xi_{f0} = 0.0875$ so as not to violate the condition of continuity of flux at the initial time $\tau = 0$. The simulation interval τ_p had to be adjusted so that the lagging end of the solute distribution (at $\xi = 0.0275$) convected through to the front (see figure captions). The value of $\delta\xi_{f0}$ for the broader transition zone is thus 0.06. Comparison with profiles in Figs. 8 and 9 respectively shows that, all other parameters being held constant, the peak height decreases with an increase in the transition zone thickness. To study the effect of the operational parameters, we maintained the transition zone of

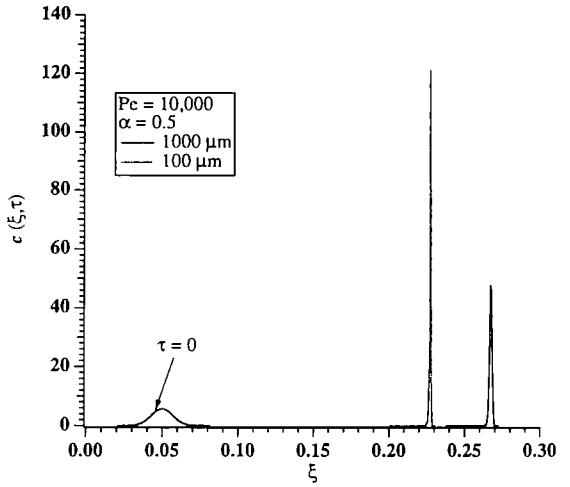

Figure 11. Same as Fig. 10, but for a reference anisotropy of 0.50. The simulation interval τ_p is 0.2 for a transition zone thickness of 100 μm and 0.24 for that of 1000 μm.

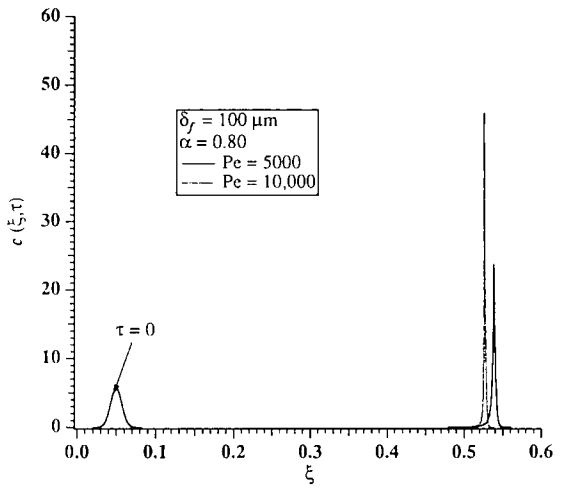

Figure 12. Effect of the Péclet number. The reference anisotropy of the medium is 0.80. The front moves with a velocity that is the arithmetic mean between the upstream and downstream values for the solute. The concentration profile corresponding to Pe = 5000 has been shifted slightly to the right for clarity.

thickness 100 μm while decreasing the Pe by a factor of half. The resultant peaks for the solute are plotted in Figs. 12 and 13. It can be seen that the concentration profile is much broader for the lower Pe. The scaling of the peak height with the transition zone thickness and the Pèclet number is discussed in detail in the next section.

Pairwise comparison of Figs. 8-9, 10-11, and 12-13 indicates that as the material becomes more anisotropic

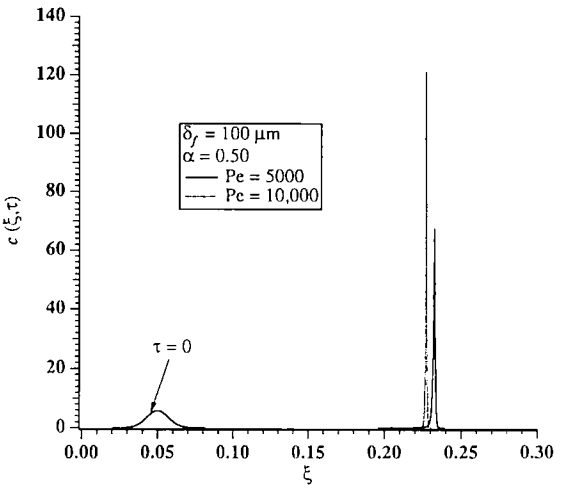

Figure 13. Same as Fig. 12, but for a reference anisotropy of 0.50.

(α changes from 0.80 to 0.50), the enhancement in concentration obtained increases. For a change of 37% in α, the height of the peak increased by a factor of 2.6, 1.9, and 2.8 respectively. Hence the need to synthesize high anisotropy, low response time LC materials.

5. Discussion

5.1. *Stationary Front*

The simple static situation of steady convection diffusion through a stationary interface exhibits the key physical feature that the thickness of the transition in solute concentration is considerably wider than the $O(1/\mathrm{Pe})$ thickness arising in a discontinuous medium, and coincides precisely with the front in material properties in the limit of large Péclet number. The experiments show a broader tail which apparently extends substantially beyond the gel front. This phenomenon is a subject of current investigation.

5.2. *Moving Front*

Figures 6 and 7 illustrate the change in concentration profile of the solute made to continuously experience the presence of a front that is moving with a velocity equal to its downstream velocity ($\beta_f = \alpha$). We observe that the final concentration distribution, at $\tau_p = 0.25$ and 0.1 respectively, is substantially narrower than the initial Gaussian distribution. The moving front has thus introduced an anti-dispersive effect on the transport of the solute. Starting at time $\tau = 0$, we note

that the concentration profile becomes progressively sharper for about 75% of the total interval simulated, after which the height of the peak starts to decrease. Moreover, for large times, the peaks become asymmetric with considerably greater dispersion on the downstream side than the upstream side. This is an undesirable effect from a focusing and purification standpoint. When the front is moved with a velocity equal to the downstream velocity of the solute, the velocity of the solute relative to the front on the downstream side becomes zero. The convective driving force for solute accumulation from the downstream side ($v^{II} - v_f$) vanishes. Diffusional effects—though small—do exist, and in the absence of the convectional driving force they cause solute dispersion on the downstream side. This decreases the maximum value of the concentration. In the domain upstream of the interface, convectional driving force is very large and dominates over diffusion leading to a much smaller spread of the solute near the interface.

The decrease in peak height over large times can be overcome by choosing the front velocity to be greater than the downstream velocity (but less than the upstream value). This choice produces a convective driving force towards the front on the downstream side, preventing downstream dispersion. Figures 8 and 9 show the results when the front was made to move at a speed that is the arithmetic mean of the upstream and downstream velocities of the solute ($\beta_f = (1+\alpha)/2$). The problem of decrease in peak height has thus been rectified at the cost of the higher time required for concentrating the solute (see Eq. (19)).

Figures 12 and 13, which compare concentration profiles for Pe = 5000 and 10,000, indicate that the peak width decreases as the Péclet number increases. However, the peak widths observed are considerably larger than $O(1/\mathrm{Pe})$ expected on the basis of boundary layer analysis for discontinuous media. The magnitude of the peak widths observed in Figs. 12 and 13 suggest that they scale as $1/\sqrt{\mathrm{Pe}}$; this may be qualitatively explained as follows. In the absence of diffusion, convection of solute toward the front would produce an infinitesimally thin (and infinitesimally high) peak at long times. This structure is centered as $x = L_f(t)$, where the solute velocity relative to the front is locally linear,

$$v(x,t) - v_f \sim (\text{constant})(x - L_f), \qquad (26)$$

given the finite width of the front (cf. Eq. (6)). When diffusion acts to spread out the peak, it is balanced by a convective flow toward $x = L_f$ that is weak in the sense that it vanishes as $x \to L_f$. Thus, relative to the case of convection with uniform velocity toward $x = L_f$ (as for a discontinuous medium), convection is less effective at concentrating the solute, hence the greater peak width (and smaller height). Detailed arguments will be presented elsewhere to explain when the appropriate scaling is precisely with $\sqrt{\mathrm{Pe}}$ (Vaidya et al., 1996). Diffusion sets an $O(1/\sqrt{\mathrm{Pe}})$ limit on the degree to which the solute peak can be sharpened. (There may be another practical limitation to minimizing the width of the concentrated peaks. When an electrically charged solute continually piles up against the interface, its concentration decreases the local voltage gradient. As the concentration increases in the boundary layer, it may reach a limiting value at which the voltage gradient may become close to zero. The electrophoretic velocity of the solute would vanish locally and thus prevent further enhancement in the height of the solute peak. The solute would then form a flat band at the limiting value of the concentration.)

It is worth noting that any factor that increases the gradient in v at the front (either a decrease in α or a decrease in δ_f) enhances the strength of convection toward the surface $x = L_f$, because it increases the constant in Eq. (26). This strong convective driving force is, of course, balanced by diffusion. Thus, at a given Pe, the concentration of solute peak height should increase with decrease in α and δ_f. This trend can, in fact, be observed by comparing Figs. 11 and 12.

6. Conclusion

A space and time varying strategy based on tunability of LC molecules for enriching a solute at a moving front has been discussed. This anti-dispersive effect on concentration peaks is relevant for amplification of low-level signal from solutes present in trace quantities, in order to facilitate their detection and isolation in analytical separations. As noted in the introduction, tunable media in real life will not literally have piecewise constant transport properties—the discontinuous case to which most of the previous work (Ramkrishna and Amundson, 1974; Locke and Arce, 1993a; Locke et al., 1993) applies—but rather would have fronts of small but finite thickness. We have shown that this finite thickness dramatically affects the dynamics of solute concentration at a moving front. In particular, it seems to set a $O(1/\sqrt{\mathrm{Pe}})$ limit on the peak width, which is very different from

the $O(1/\mathrm{Pe})$ width applicable to a truly discontinuous medium.

Detailed scaling analysis of the large Péclet number solute concentration near a moving front will be presented elsewhere (Vaidya et al., 1996). Future experimental efforts will aim to demonstrate the actual practical implementation of this technique. Another step would be to explore the concept of flow through tunable materials that adsorb solute. Theoretical modeling of this problem would proceed by addition, on the right-hand side of Eq. (1), of a reaction term with rate constants that can vary with time as well as position along the column.

Scale-up considerations are limited at this stage due to power costs and safety considerations stemming from the existence of electric fields. However, it has potential for separation and enrichment of ionizable gas. In this case, in spite of high voltages there would be low currents, keeping power costs low and safety hazards minimum. The success of this technique will depend on the synthesis of adequately anisotropic LC materials.

Nomenclature

c	Concentration of solute	kg/m^3
D	Diffusion coefficient	m^2/s
f	Initial concentration distribution	kg/m^3
K_{eq}	Equilibrium constant, dimensionless	
L	Length of column	m
L_f	Location of interface from column entrance	m
Pe	Péclet number, dimensionless	
t	time	s
v	Velocity	m/s
x	Lab-fixed spatial coordinate	m

Greek Letters

α	Anisotropy of reference solute, dimensionless	
β_f	Ratio of the front velocity to the reference velocity, dimensionless	
η	Coordinate in the transition zone, dimensionless	
ϵ	Inverse Péclet number, dimensionless	
ϕ	Dimensionless diffusion coefficient	
μ	Dimensionless velocity	
σ	Standard deviation of Gaussian distribution	m
τ	dimensionless time	
θ	Orientation angle of LC molecules	radians
ξ	Dimensionless lab-fixed spatial coordinate	

Superscripts

-	Reference values
i	Upstream or downstream domain
I	Upstream domain
II	Downstream domain

Subscripts

$\parallel$	Parallel (fast) mode
$\perp$	Perpendicular (slow) mode
∞	Far away from the interface
f	Interface
0	At time $t = 0$
sing	Singular front

Acknowledgments

The authors gratefully acknowledge support of this research by the National Science Foundation through the Presidential Young Investigator Program (D.A.K.) and National Young Investigator Program (J.M.N. and S.L.D.), as well as National American Heart Association Grant-in-Aid 93-8670 (S.L.D.).

References

Bhaskar, R.K., R.V. Sparer, and K.J. Himmelstein, "Effect of an Applied Electric Field on Liquid Crystalline Membranes: Control of Permeability," *J. Membrane Sci.*, **24**, 83–96 (1985).

Brenner, H., "The Diffusion Model of Longitudinal Mixing in Beds of Finite Length. Numerical Values," *Chem. Engng Sci.*, **44**, 827–840 (1962).

Brzezinski, W., W.M.J. van Gelder, P. Mendelewski, and P. Kolster, "Polyacrylamide Gel Electrophoresis of Wheat Gliadins: The Use of a Moving Boundary for Improved Resolution," *Euphytica*, **40**, 207–212, (1989).

Chrambach, A., "Unified View of Moving Boundary Electrophoresis: Practical Implications (Plenary Lecture)," *J. Chromatogr.*, **320**, 1–14, (1985).

Chu, G., D. Vollrath, and R.W. Davis, "Separation of Large DNA Molecules by Contour-Clamped Homogeneous Electric Fields," *Science*, **234**, 1582–1585 (1986).

Danckwerts, P.V., "Continuous Flow Systems. Distribution of Residence Times," *Chem. Engng Sci.*, **2**, 1–18, (1953).

de Gennes, P.G. and J. Prost, *The Physics of Liquid Crystals* (2nd Ed.), Clarendon Press, Oxford, 1993.

Deinhammer, R.S., E.-Y. Ting, and M.C. Porter, "Dynamic Modification of Separations Using Electrochemically Modulated Liquid Chromatography," *Anal. Chem.*, **67**, 237–246 (1995).

Gallagher, S.R. and J.A. Smith, *Current Protocols in Molecular Biology*, John Wiley and Sons Inc., **2**, 10.2.19, 1993.

Ghatak-Roy, A.R. and C.R. Martin, "Electromodulated Ion Exchange Chromatography," *Anal. Chem.*, **58**, 1574–1575 (1986).

Grimshaw, P.E., A.J. Grodzinsky, M.L. Yarmush, and D.M. Yarmush, "Dynamic Membranes for Protein Transport: Chemical and Electrical Control," *Chem. Engng. Sci.*, **44**, 827–840 (1989).

Ivory, C.F. and W.A. Gobie, "Continuous Counteracting Chromatographic Electrophoresis," *Biotechnol. Prog.*, **6**, 21–32 (1990).

Krüger, G.J., "Diffusion in Thermotropic Liquid Crystals," *Phys. Rep.*, **82**(4), 229–269 (1982).

Leonard, B.P., "A Stable and Accurate Convective Modelling Procedure Based on Quadratic Upstream Interpolation," *Comp. Meth. Appl. Mech. Eng.*, **19**, 59–98 (1979).

Locke, B.R. and P. Arce, "Applications of Self-Adjoint Operators to Electrophoretic Transport, Enzyme Reactions, and Microwave Heating Problems in Composite Media-I. General Formulation," *Chem. Engng Sci.*, **48**, 1675–1686 (1993a).

Locke, B.R., P. Arce, and Y. Park, "Applications of Self-Adjoint Operators to Electrophoretic Transport, Enzyme Reactions, and Microwave Heating Problems in Composite Media-II. Electrophoretic Transport in Layered Membranes," *Chem. Engng Sci.*, **48**, 4007–4022 (1993).

Ly, Y. and Y.-L. Cheng, "Electrically-Modulated Variable Permeability Liquid Crystalline Polymeric Membrane," *J. Membrane Sci.*, **77**, 99–112 (1993).

Moseley, M.E. and A. Loewenstein, "Anistropic Translational Diffusion of Methane and Chloroform in Thermotropic Nematic and Smectic Liquid Crystals," *Mol. Cryst. Liq. Cryst.*, **90**, 117–145 (1982).

Muralidhara, H.S., "Enhance Separations with Electricity," *Chemtech*, **24**(5), 36–41 (1994).

Novy, R.A., H.T. Davis, and L.E. Scriven, "Upstream and Downstream Boundary Conditions for Continuous-Flow Systems," *Chem. Engng. Sci.*, **45**, 1515–1524 (1990).

O'Farrell, P.H., "Separation Techniques Based on the Opposition of Two Counteracting Forces to Produce a Dynamic Equilibrium," *Science*, **227**, 1586–1589 (1985).

Prasad, R., F. Notaro, and D.R. Thompson, "Evolution of Membranes in Commercial Air Separation," *J. Membrane Sci.*, **94**, 225–248 (1994).

Sauer, S.G., B.R. Locke, and P. Arce, "Effects of Axial and Orthogonal Applied Electric Fields on Solute Transport in Poiseuille Flows. An Area Averaging Approach," *Ind. Eng. Chem. Res.*, **34**, 886–894 (1995).

Raj, C.B.C., "Protein Purification by Counteracting Chromatographic Electrophoresis: Quantitative Focusing Limits and Protein Selection at the Interface," *J. Biochem. Biophys. Methods*, **28**, 161–172 (1994).

Ramakrishna, D. and N.R. Amundson, "Transport in Composite Materials: Reduction to a Self Adjoint Formalism," *Chem. Engng Sci.*, **29**, 1457–1464 (1974).

Vaidya, D.S., J.M. Nitsche, S.L. Diamond, and D.A. Kofke, "Convection-Diffusion of Solutes in Media with Piecewise Constant Transport Properties," in print, *Chem. Engng. Sci.* (1995).

Vaidya, D.S., J.M. Nitsche, S.L. Diamond, and D.A. Kofke, "Separations in Tunable Media," in preparation. *AIChE. J.*, (1996).

Winnick, J., "Electrochemical Membrane Separations," *Chem. Eng. Prog.*, **86** (1), 41–46 (1990).